Neuron
Article

Cytosolic Transmitter Concentration Regulates Vesicle Cycling at Hippocampal GABAergic Terminals

Lu Wang,[1,2,3,4,5,7] Peng Tu,[1,2,3,7] Laurine Bonet,[1,2,3] Karin R. Aubrey,[1,2,3,6] and Stéphane Supplisson[1,2,3,*]
[1]INSERM, U1024, F-75005 Paris, France
[2]CNRS, UMR 8197, F-75005 Paris, France
[3]Ecole Normale Supérieure, Institut de Biologie de l'ENS, IBENS, F-75005 Paris, France
[4]Shanghai Key Laboratory of Brain Functional Genomics, East China Normal University, 200062 Shanghai, China
[5]Present address: Institute of Neuroscience and State Key Laboratory of Neuroscience, Shanghai Institutes for Biological Sciences, Chinese Academy of Sciences, 200031 Shanghai, China
[6]Present address: Pain Management Research Institute, Kolling Institute of Medical Research, Northern Clinical School, University of Sydney at Royal North Shore Hospital, Sydney, NSW 2065, Australia
[7]These authors contributed equally to this work
*Correspondence: stephane.supplisson@biologie.ens.fr
http://dx.doi.org/10.1016/j.neuron.2013.07.021

SUMMARY

Sustained synaptic transmission requires vesicle recycling and refilling with transmitter, two processes considered to proceed independently. Contrary to this assumption, we show here that depletion of cytosolic transmitter at GABAergic synapses reversibly reduces the number of recycling vesicles. Using paired recordings in hippocampal cultures, we show that repetitive activity causes two phases of reduction of the postsynaptic response. The first involves the classical depletion of the readily releasable and recycling pools, while the second reflects impairment of vesicle filling as GABA is consumed, since it can only be reversed by uptake of GABA or its precursors, glutamate or glutamine. Surprisingly, this second phase is associated with reduced quantal release, a faster depression rate and lower FM5-95 labeling, suggesting that the size of the cycling vesicular pool is regulated by cytosolic transmitter availability. Regulation of vesicular cycling may represent a general mechanism of presynaptic plasticity, matching synaptic release to transmitter supply.

INTRODUCTION

Information transfer between neurons requires a precise temporal and spatial balance of excitatory and inhibitory synaptic inputs. In the hippocampus, inhibitory interneurons, which represent ~10% of the total neuronal population, are able to shape the network activity of large cellular ensembles by releasing GABA at high frequency along extensive axonal arborizations (Klausberger et al., 2003). Since small central synapses contain a limited set of vesicles, release sites, and transmitters, several recycling schemes cooperate to maintain a pool of GABA-filled vesicles available for release (Edwards, 2007; Kraushaar and Jonas, 2000; Neher, 2010; Sara et al., 2002; Südhof, 2004).

Vesicle trafficking and pools have been studied in great detail (Kavalali, 2006; Rizzoli and Betz, 2005; Rizzoli and Jahn, 2007; Südhof, 2004) but much less is known about where and how vesicles are filled with GABA via VIAAT (also named VGAT), the shared vesicular transporter for GABA and glycine (Aubrey et al., 2007; Wojcik et al., 2006). After exocytosis, vesicles retrieved by clathrin-mediated endocytosis are rapidly acidified (Atluri and Ryan, 2006) and recycled either directly or through endosomes (for review see Rizzoli and Jahn, 2007; Südhof, 2004). Direct recycling implies that filling may be interrupted before its completion if partially filled vesicles are recruited for release. In addition, the time course of GABA accumulation should be sensitive to variation in VIAAT copy number and VIAAT occupancy. In contrast, vesicles processed through larger VIAAT-containing acidic endosomes may be more homogeneously preloaded with GABA before burgeoning.

Manipulations that alter GABA metabolism have been shown to change the amplitude of evoked and miniature IPSCs in brain slices, suggesting that the amount of GABA stored in vesicles is regulated (Barberis et al., 2004; Engel et al., 2001). However, it has proven difficult to dissect the relative contribution of different supply sources: diffusion from the cell body reservoir, capture by transporters located in axon and terminal membranes, and de novo synthesis from glutamate by the two isoforms of glutamate decarboxylase (GAD65 and GAD67). Although genetic invalidation in knockout mice has identified GAD67 and VIAAT as the two critical elements for the vesicular release of GABA (Asada et al., 1997; Wojcik et al., 2006), membrane-anchored GAD65 is important for GABA synthesis during intense synaptic activity (Tian et al., 1999; Walls et al., 2011). The role of presynaptic plasma membrane transporters for maintaining GABA homeostasis and vesicle filling is less understood, although there is evidence that glutamate and glutamine uptakes potentiate GABAergic IPSCs in brain slices and cultures (Bak et al., 2006; Brown and Mathews, 2010; Ertunc et al., 2007; Fricke et al., 2007; Mathews and Diamond, 2003).

Here, we consider the reversible and irreversible changes that occur in inhibitory signaling while neurons are continuously firing and actively consuming transmitter. In contrast to the well-described depression caused by vesicle depletion (Kraushaar

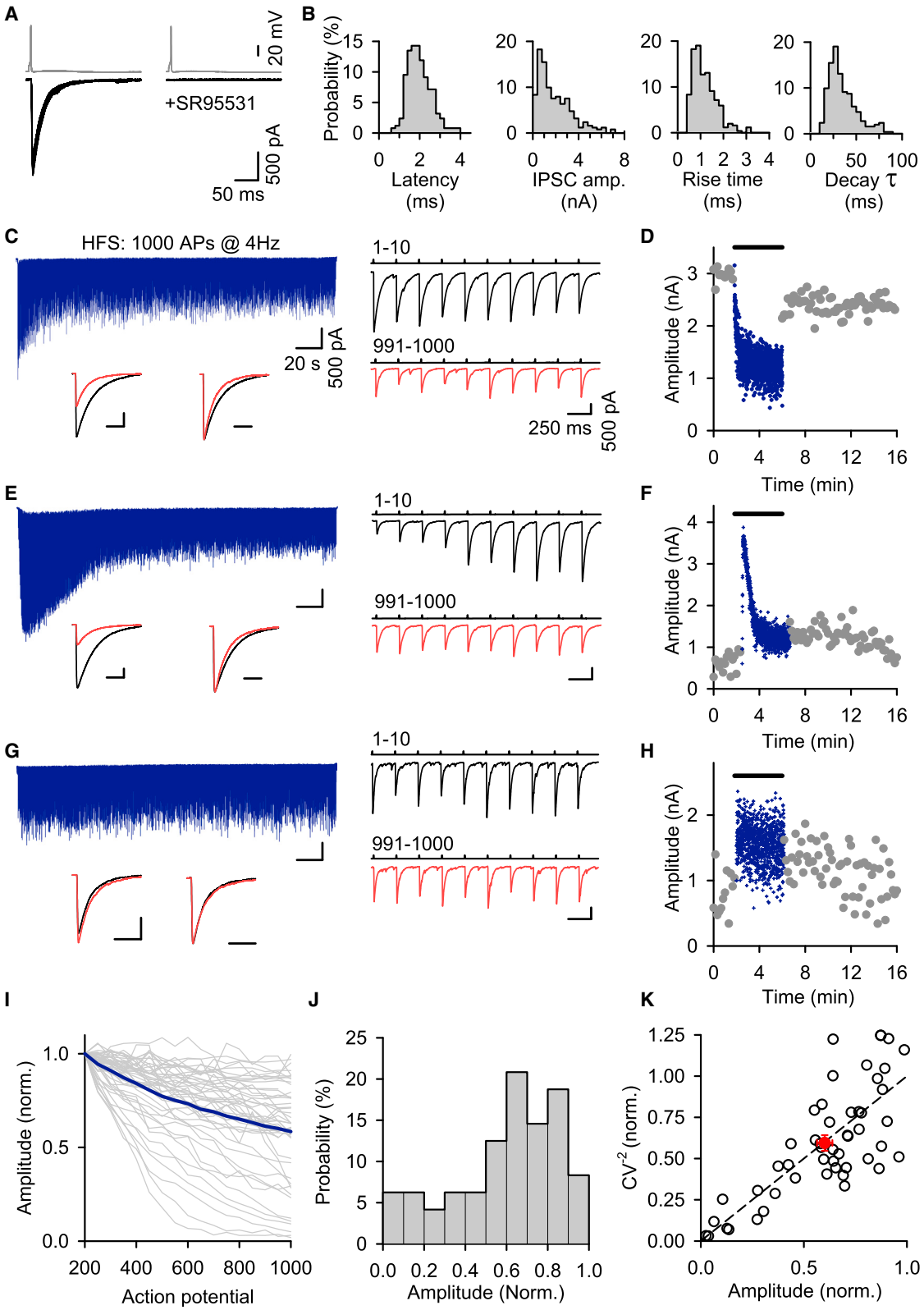

Figure 1. Vesicle Recycling Supports Steady GABA Release during Repetitive Stimulation

(A) Sample traces of IPSCs (bottom) evoked by ten APs (top) at 0.1 Hz in pairs with a presynaptic GAD65(+) cell in control condition (left) and in the presence of 20 μM SR95531 (right).

(legend continued on next page)

and Jonas, 2000; see review in Zucker and Regehr, 2002), we show that GABA consumption induces a collapse of transmission that is only restored by GABA, glutamate, and glutamine transporter-mediated uptake. Changes in kinetic and quantal parameters during transmission rundown suggest a decrease in the pool of neurotransmitter-containing vesicles available for release, and FM5-95 uptake confirmed reduced vesicle trafficking in transmitter-depleted terminals. This cytosolic GABA regulation of vesicle cycling represents a previously uncharacterized form of presynaptic plasticity.

RESULTS

Vesicle Recycling Maintains the Strength of Inhibition during Repetitive Activity

We identified inhibitory neurons by fluorescence in hippocampal cultures derived from transgenic EGFP-GAD65 mice. Putative pairs composed of a GAD65(+) presynaptic element and a nearby nonfluorescent postsynaptic cell were whole-cell patched in current- and voltage-clamp modes, respectively, and tested for synaptic connection by injecting depolarizing current steps that triggered action potentials (APs) in the presynaptic cell (Figure 1A). The probability of connection was high (>90%) and the evoked inhibitory postsynaptic currents (IPSCs) were entirely blocked by SR95531 (20 μM), a specific $GABA_A$ receptor inhibitor (Figure 1A). The connections were monosynaptic, as indicated by the absence of transmission failures and the short latency (2.0 ± 0.04 ms, n = 252, Figure 1B). With high intracellular Cl^-, typical inward IPSCs had large amplitude (2.04 ± 0.11 nA, n = 252, Figure 1B), when recorded in cells held at −70 mV, and fast kinetics, with a 20%–80% rise time of 1.17 ± 0.03 ms and a decay time constant of 35.3 ± 0.99 ms (n = 252, Figure 1B).

We first set out to evaluate whether transmission could be maintained during repetitive stimulation in the absence of an exogenous mechanism for GABA supply. We recorded IPSCs during long trains of 500–2,000 APs evoked at 4 Hz, a moderate frequency with rare AP failures (0.8% ± 0.08% failure, n = 88 pairs). Repetitive stimulation triggered a broad range of short-term synaptic plasticities, which were always followed by a long-lasting phase of relatively steady release, indicating that newly formed GABA-containing vesicles are at equilibrium with vesicle exocytosis. Figure 1 shows this long phase of steady release for three representative pairs displaying initial short-term depression (Figures 1C and 1D), facilitation followed by depression (Figures 1E and 1F), or stable responses (Figures 1G and 1H). On average, IPSC decay kinetics were slightly faster by the end of the train (insets, 32.6 ± 1.7 ms at the beginning [black trace] and 28.4 ± 1.3 ms at the end of the train [red trace], n = 63 pairs, p = 0.05). To compare the late phase of release for all tested pairs, we averaged the peak amplitude by groups of 50 consecutive IPSCs normalized by the value at the 200th AP, after initial facilitation and/or depression. Figure 1I shows the amplitude change during the last 800 APs for individual (gray line) and average (solid line) pairs. The final IPSC amplitude was maintained at 62.5% ± 3.5% (n = 48, p < 0.001, Figures 1I and 1J), indicating robust recycling activity in a majority of pairs. The linear relationship between the normalized inverse of the square of the coefficient of variation (CV^{-2}) and the IPSC amplitude was compatible with a presynaptic locus for this slow depression (Figure 1K).

These results confirm that the initial cytosolic stock of GABA that had been built up for days in glutamine-enriched culture media supports the filling of rapidly recycling vesicles in the absence of exogenous GABA supply.

Sustained Vesicle Recycling Collapses Transmission in the Absence of Exogenous GABA Supply

Despite the existence of a pseudo steady-state described above, multiple repetitions of the 4 Hz train every 10 min induced a gradual but near complete rundown of GABA transmission as shown in Figure 2A. After five consecutive 500 AP trains, the maximal IPSC amplitude was reduced by 96.3% (from 1,000 ± 36 pA to 37.5 ± 2.5 pA), and the cumulative amplitude by 99% (Figure 2B). Impairment in vesicle recycling or vesicle filling with GABA was indicated by the reduction in steady release observed during the third and subsequent 4 Hz trains (Figures 2C and S1 available online). This reduction was maintained even if the stimulation frequency was reduced to 0.1 Hz (Figure 2A, gray circle and Figure S2). Rundown was present for depressing (Figure 2A) and facilitating synapses (Figure S3) and also developed by continuous stimulation at 1 Hz (Figure S3), with linear CV^{-2}-IPSC relationship (Figure S3; slope = 1.05, r^2 = 0.89, n = 59), in agreement with a presynaptic origin.

To examine whether the time of whole-cell dialysis or the number of synaptic events was critical for this rundown, we increased the number of APs delivered per train, from 500 to 1,000 and occasionally up to 4,000 APs. Longer trains were often associated with a biphasic time course for the rundown, as shown in Figures 2D and 2E. The linear cumulative amplitude for the first and second train (r^2 = 1.00, Figure 2F) suggests that the recycling capacity was initially able to match release, until an imbalance appeared during the third train and transmission eventually collapsed (Figures 2D, 2E, and 2F). We compared the time (Figures 2D and 2G) and AP number (Figures 2E and 2H) that achieved 90% reduction in cumulative amplitude (t_{90}, AP_{90}, respectively) for trains of 500 (blue line) and 1,000 (brown line) APs. There was a significant decrease in t_{90}, from 48.8 ± 3.5 min (500 APs/train, n = 16) to 29.4 ± 2.6 min (1,000 APs/train,

(B) Probability distribution histograms for IPSC latency, amplitude, rise time, and decay time constant (n = 252).
(C, E, and G) Steady GABA release triggered by 1,000 APs at 4 Hz. Left: sample IPSCs traces having (C) short-term depression; (E) facilitation followed by short-term depression; (G) stable release probability. Right: traces of IPSCs at the onset (black) and at the end (red) of the sample in the left panel. Insets: average (left) and peak scaled (right) traces of IPSCs in the right panel, same colors. Horizontal bars represent 50 ms; vertical bars represent 500 pA.
(D, F, and H) Peak amplitude evoked at 0.1 Hz (gray circles) and at 4 Hz (blue crosses) for the pairs described in (C), (E), and (G), respectively.
(I) Individual (gray line) and average (blue line, n = 50) time courses of IPSC amplitude between 200 and 1,000 APs, normalized by the value at the 200th AP.
(J) Probability distribution of the steady amplitude (APs: 951–1,000) normalized by the amplitude at the 200th AP (n = 50).
(K) Normalized changes in CV^{-2} and mean amplitude between 200 and 1,000 APs (open circles, red circle: mean ± SEM).

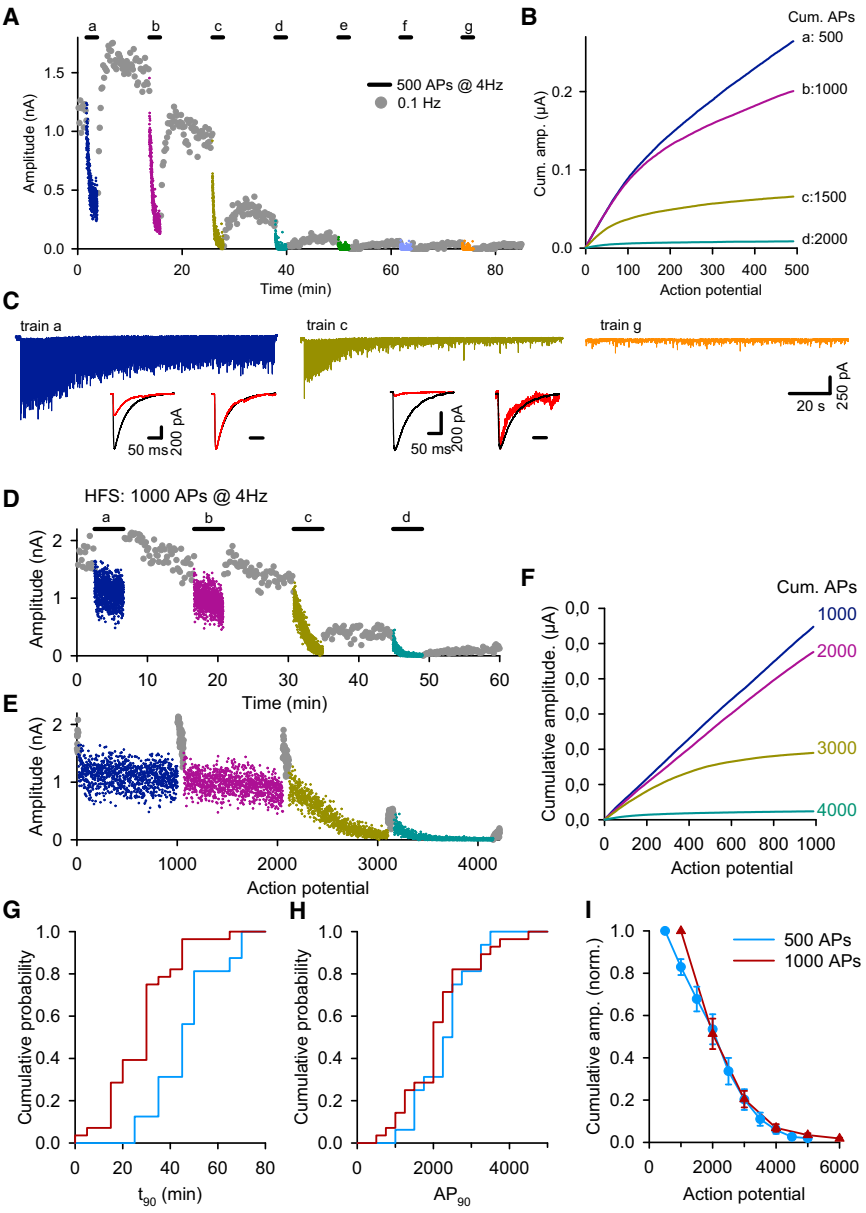

Figure 2. Sustained Activity Induces a Complete Rundown of GABAergic Transmission

(A) Rundown of IPSC amplitude evoked during seven 4 Hz trains (500 AP/train; bars a to g; crosses with different colors).

(B) Cumulative amplitude for the trains (a to d) shown in (A).

(C) IPSCs traces of the (a) (left), (c) (middle), and (g) (right) 4 Hz trains. Inset: average (left) and peak scaled (right) IPSCs at onset (APs: 1–10, black line) and end (APs: 491–500, red line) of the train.

(D and E) IPSC amplitude evoked at 0.1 Hz (gray circles) and 4 Hz (solid bars, four trains of 1,000 APs labeled a to d) plotted as function of time (D) or AP number (E) for a cell with biphasic rundown.

(F) Cumulative amplitude for the trains (a) to (d) shown in (D).

(G and H) Cumulative probability of the time (t_{90}) and number of APs (AP_{90}) needed to reach 90% of the cumulative IPSC peak amplitude for pairs stimulated with trains of 500 (light blue line, n = 15) and 1,000 APs (dark red line, n = 21).

(I) Cumulative amplitude ± SEM for 4 Hz trains of 500 (light blue, n = 15) and 1,000 APs (dark red, n = 21) normalized by the value of the first train. See also Figures S1, S2, S3, and S4.

n = 28; p < 0.001), whereas AP_{90}s were similar: 2,408 ± 171 APs (n = 16) and 2,245 ± 173 APs (n = 28, p = 0.54, Figure 2H). The 19.4 min difference for the 500 APs/train can be accounted for by the two additional resting periods of 10 min needed to achieve the same number of APs as in the 1,000 APs/train protocol. Figure 2I shows the similar reduction in cumulative IPSC amplitude for consecutive trains when plotted as function of AP number.

After transmission collapse, the amplitude of the current evoked by bath application of 10 µM GABA remained stable (92% ± 6%, n = 3; Figure S4), indicating unchanged membrane expression of $GABA_A$ receptors. Together, these results suggested that in the absence of exogenous GABA supply, sustained vesicular release was the key factor contributing to transmission rundown.

Diffusion of Transmitters from the Cell Body Partially Maintains Recycling Activity

To examine whether depletion of presynaptic GABA was the cause of rundown, we added GABA or glutamate to the presynaptic pipette. Figure 3 shows reduced rundown for representative cells patched with a pipette containing GABA (10 mM; Figures 3A and 3B) or glutamate (20 mM; Figures 3C and 3D). In control neurons, the cumulative amplitude for trains recorded after ~3,000 APs decreased to 7.3% ± 1% (n = 44) of the initial value, whereas IPSC amplitude was maintained after 6,000 APs when the pipette solution contained GABA (43.7% ± 9.1%, n = 6, p < 0.001) or glutamate (62.5% ± 11%, n = 8, p < 0.001). We used the cumulative IPSC amplitude normalized by the initial amplitude (i.e., the equivalent number of full size IPSC [fsIPSC]) as a proxy for GABA release. In control conditions, the cumulative amplitude reached a plateau of 970.4 ± 71 fsIPSCs (n = 44; Figures 3E and 3F) and half of this maximum was achieved after 1,063 ± 73 APs (n = 44). In contrast, Figures 3E and 3F show that when GABA or glutamate was present in the presynaptic pipette solution, the cumulative amplitude was still increasing after 6,000 APs, reaching 2,904 ± 540 fsIPSCs for GABA (10–20 mM, n = 6, p < 0.001) and 2,637 ± 358 fsIPSCs for glutamate (20 mM, n = 8, p < 0.001). These results demonstrate that rundown is primarily caused by the loss and consumption of a finite stock of presynaptic GABA.

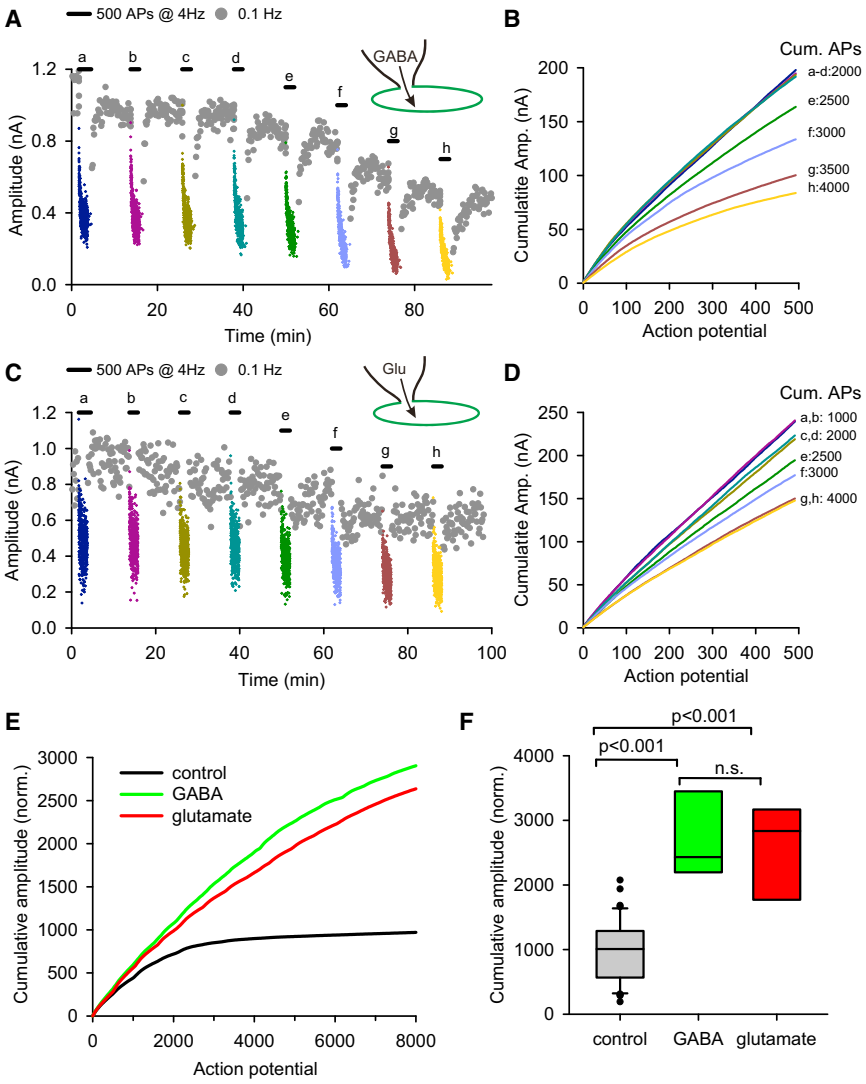

Figure 3. Somatic Supply of GABA or Glutamate Maintains Vesicle Recycling

(A) IPSC evoked by the same protocol as in Figure 2A but with GABA (10 mM) added to the presynaptic pipette solution.

(B) Cumulative amplitude for the eight trains in (A).

(C) Same as in (A) but with glutamate (20 mM) and 200 μM PLP added in the pipette solution.

(D) Cumulative amplitude for the eight trains in (C).

(E) Average cumulative IPSC amplitude for repeated trains normalized by the initial IPSC amplitude in control (black line, n = 20) or in the presence of GABA (10–20 mM, green line, n = 4) or glutamate (20 mM with 200 μM PLP, red line, n = 5).

(F) Box plot showing the distribution of the final cumulative IPSC amplitude normalized by the initial amplitude with the same pairs as in (E). Mann-Whitney U test.

Three Neuronal Transporters Restore Vesicle Recycling in GABA-Depleted Neurons

To examine how uptake via neuronal transporters supports VIAAT-mediated vesicle loading, we first GABA depleted neuronal pairs by repeated stimulation with 4 Hz trains until the IPSC amplitude was <10% of the initial value (data not shown). We then added GABA (100 μM; Figure 4A), glutamate (50 μm; Figure 4B), or glutamine (2 mM; Figure 4C) to the extracellular solution and examined whether uptake could restore vesicular release and transmission. GABA and glutamate were applied in the presence of high concentrations of specific receptor inhibitors to avoid tonic activation of GABA and glutamate receptors.

The three uptake systems similarly restored synaptic release of GABA as indicated by the large potentiation in IPSC amplitude (Figures 4A–4C). On average, the normalized IPSC peak amplitude showed a 15-fold potentiation at 0.1 Hz, from 6.4% ± 0.9% in depleted cells to 94% ± 1.6% after a single GABA application (n = 7, p = 0.002; Figure 4G). Glutamate uptake restored a smaller fraction of the initial amplitude (from 4.8% ± 0.8% in depleted neurons to 66.5% ± 6% after glutamate, n = 9, p < 0.001; Figure 4G). Surprisingly, uptake of glutamine, which requires two enzymatic transformations to produce GABA, induced a similar fast and complete recovery of IPSC amplitude (from 6.4% ± 1.5% in depleted neurons to 101% ± 18.3% after glutamine, n = 16, p < 0.001; Figure 4G). Furthermore, GABA uptake restored the initial capacity of presynaptic neurons to support release during long stimulus train, as the cumulative IPSC amplitude after GABA application was comparable to the initial 4 Hz train (95.3% ± 7%, n = 8, p < 0.001; Figures 4D and 4E). In contrast, lower cumulative amplitudes were observed after glutamate (67.3% ± 5%, n = 8, p < 0.001; Figures 4D and 4E) or glutamine (69.4% ± 9%, n = 15, p < 0.001; Figures 4D and 4E) uptake, suggesting a smaller buildup of presynaptic GABA stores via these transporters.

To verify that the restorations were the result of transporter-mediated uptake, we applied GABA (10 μM) in the presence of SKF-89976 (20 μM), a specific GAT1 inhibitor (Figure 4F). There was no significant increase in IPSC amplitude after washout: 6.9% ± 2.8% in depleted cells and 6.2% ± 2.7% in the presence of SKF-89976 (n = 5, n.s.; Figure 4G). Similarly there was no restoration when glutamate (20 μM) was applied in the presence of the EAAT1–EAAT3 inhibitor TFB-TBOA (4 μM), with relative amplitude of 6.2% ± 1.7% in depleted cells and 8.6% ± 4.2% after glutamate + TFB-TBOA (n = 6, n.s.; Figure 4G). Since SKF-89976 and TFB-TBOA are competitive inhibitors, lower concentrations of GABA (10 μM) and glutamate (20 μM) were used in these experiments; these lower concentrations were also able to effectively restore transmission (Figure 4F).

The time courses of restoration for the three amino acids had t_{20-80} of 169 ± 33 s (n = 5) for GABA, 70.4 ± 10 s (n = 5) for glutamate, and 148 ± 27 s (n = 5) for glutamine. The values for GABA

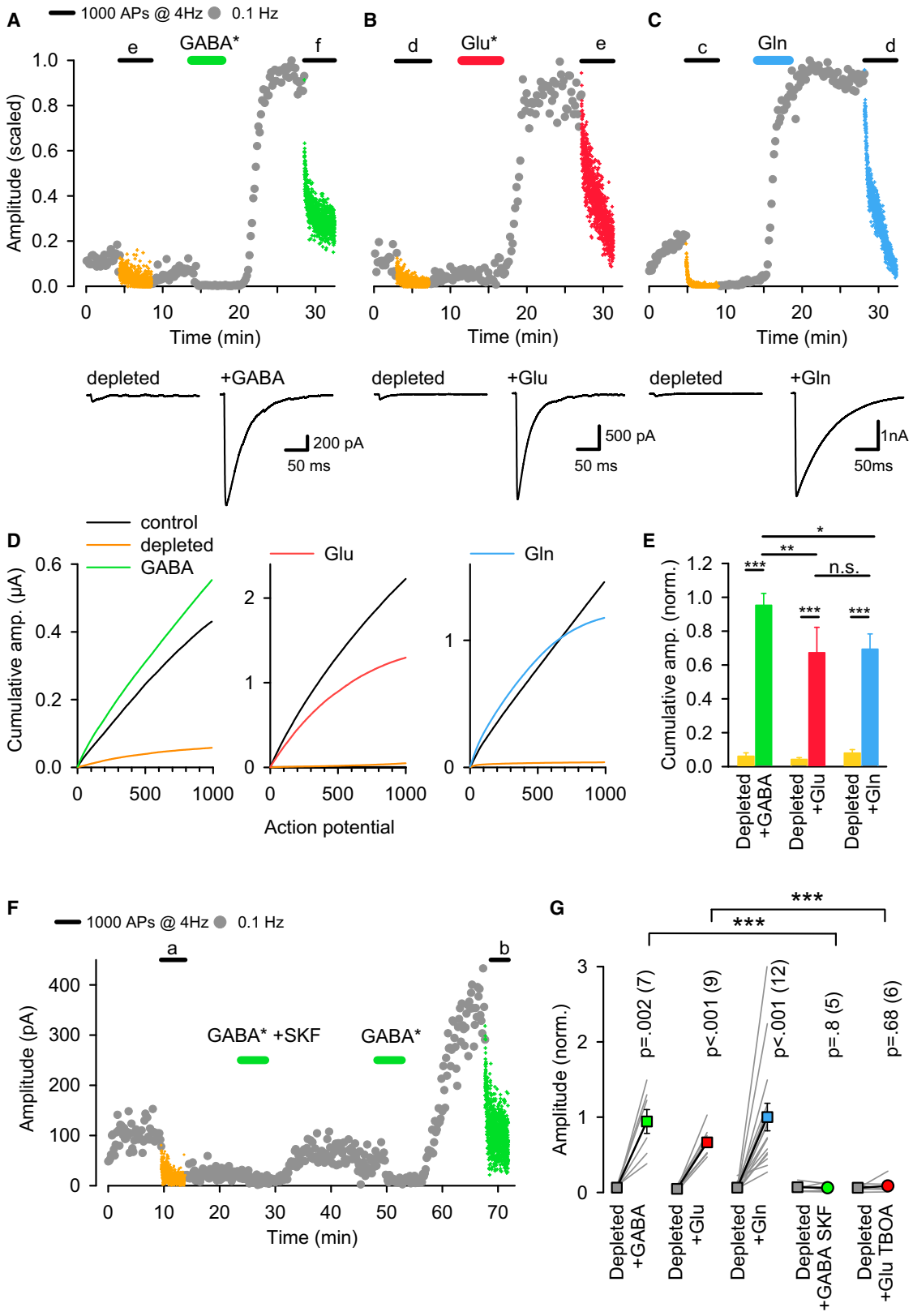

(legend on next page)

and glutamate applications were probably overestimated, as their measurement required prior washout of the receptor inhibitors.

Glutamine Uptake Directly Supports the Filling of Rapidly Recycling Vesicles

Next, we examined whether neuronal uptake of glutamine, which is the main physiological precursor for GABA synthesis, could directly support the replenishment of vesicles during repetitive activity. Figure 5A shows that continuous application of extracellular glutamine (500 μM) prevented rundown of GABA transmission, as the cumulative amplitude was maintained at 111% ± 31% (n = 8, p = 0.31; Figure 5B) of the initial value after six trains of 1,000 APs compared to 1.8% ± 0.4% in control condition (n = 21, p < 0.001; Figure 5B). The rate of glutamine uptake was not limiting for GABA supply, since increasing the glutamine concentration to 2 mM had no further effect on IPSC amplitude (Figure 5C; Cumulative Amplitude $_{Gln\ =\ 2mM}$/Cumulative Amplitude $_{Gln\ =\ 0.5mM}$ = 1.0 ± 0.06, n = 3, p = 0.841). In contrast, initiation of glutamine uptake (2 mM) during 4 Hz trains potentiated the IPSC amplitude of GABAergic neurons whole-cell patched with a pipette solution containing 20 mM glutamate (Figure 5D). On average, the cumulative amplitude increased 3.2-fold ± 0.75-fold (n = 9, p = 0.025), suggesting that glutamine transporters supply recycling vesicles with a more readily available GABA source than glutamate diffusion along the axon. Similarly, during the continuous stimulation of a GABA-depleted cell (red line), glutamine uptake restored vesicle filling and IPSC amplitude (blue line) with an average time constant of 39.3 ± 4.5 s (Figure 5E; n = 6).

To gain insight into the quantal changes induced by GABA rundown and its recovery by glutamine uptake, we plotted the CV^{-2} for the experiment shown in Figure 5E (Figure 5F). The onset of depression and its restoration by glutamine were associated with marked changes in CV^{-2}, excluding a pure effect in quantal size (q, dotted line, Figure 5F and Monte Carlo simulations in Figure S5). On the other hand, the decrease in CV^{-2} was smaller than predicted for a pure effect on release probability (p, dashed line, Figures 5F and S5) and was best fit assuming a mixed change in p by 42% and q by 58% (blue line, Figures 5F and S5).

The CV^{-2}-mean amplitude relationships shown in Figure 5G for four representative pairs confirmed a mixed change in p and q during GABA depletion with an average reduction in p of 0.54 ± 0.056 (n = 9).

Together, these results demonstrate an efficient coupling between glutamine uptake and GABA synthesis for activity-dependent vesicle filling. In addition, the p and q mixed changes suggested that GABA depletion reduced both the quantal size by decreasing the amount of GABA stored and released per vesicle and, unexpectedly, the release probability.

Cytosolic GABA Regulates Release Probability

As evidence in the literature suggested that empty vesicles continue to be released and recycled after blocking the H^+-vATPase or the vesicular transporter (Croft et al., 2005; Parsons et al., 1999; Tabares et al., 2001; Wojcik et al., 2004; Zhou et al., 2000), we examined whether alteration in vesicle filling caused by GABA depletion simply scaled down transmission. Figure 6A compares the time course of depression for six 4 Hz trains (1,000 APs; labeled a–f) and their partial recovery at 0.1 Hz for a pair with high initial release probability. The sharp reduction in amplitude during the third train suggested a decline in GABA-filled vesicle cycling, which almost vanished in later trains (d–f; Figures 6A and 6C). Uptake of extracellular glutamate (50 μM for 4 min, data not shown) restored 75% of the initial amplitude and 46% of the cumulative amplitude (labeled g; Figures 6B and 6C), confirming that the rundown was indeed caused by GABA depletion.

GABA depletion increased the paired-pulse depression (PPD) for the nine high-probability pairs analyzed (Figure 6D), and reinstating GABA supply restored the initial PPD value (Figure 6D), reinforcing the suggestion that changes in cytosolic GABA alter p. The parabolic shape of the variance-mean plot at 0.1 Hz provides further evidence for a decrease in release probability during the rundown (Figure 6E).

Although a reduction in p should slow the time course of depression, as in trains b and c (Figures 6F and 6G), we observed instead a marked transition toward faster time course after the third train (trains d–f; Figures 6F and 6G). Furthermore, reinstating GABA supply with glutamate restored p and the slow time course of depression (train g; Figures 6F and 6G). This transition toward faster kinetics in GABA-depleted neurons was present in all nine high-probability pairs analyzed (Figure 6H), with an average 51% reduction in the weighted time constant (73.1 ± 8.1 s to 37.6 ± 4.7 s, n = 9, p < 0.001, inset Figure 6H).

Because the steady release probability during long train of stimulation should be related to the pool size of recycling vesicles, we hypothesized that both phenomena, the decrease in p

Figure 4. Uptake of GABA or its Precursors Restores Transmission in Transmitter-Depleted Neurons

Neurons were stimulated with three to five trains of 1,000 APs at 4 Hz (solid bar, numbered a to e) to deplete GABA stores. Only the last 4 Hz train is shown (orange crosses) with the time origin set to 0 for clarity.

(A–C) Top: scaled amplitude of IPSCs evoked at 0.1 Hz (gray circles) or 4 Hz (1,000 APs, colored crosses). Transmission recovered after applications of (A) GABA (100 μM) in the presence of SR95531 (100 μM); (B) glutamate (50 μM) in the presence of a cocktail of GluR inhibitors (see Supplemental Experimental Procedures); and (C) glutamine (2 mM); bottom: average trace of ten IPSCs evoked at 0.1 Hz before (left) and after (right) recovery.

(D) Cumulative IPSC amplitude during trains of 1,000 APs evoked at 4 Hz for the pairs shown in (A) (left), (B) (middle), and (C) (right). The black lines correspond to the first train evoked at the onset of the recording (not shown in A–C), and the colored lines correspond to the trains shown in (A)–(C).

(E) Average + SEM cumulative IPSC amplitudes for the 4 Hz trains in GABA-depleted neurons (orange) and after application of GABA (green, n = 7), glutamate (red, n = 9), and glutamine (blue, n = 16), normalized by the first value.

(F) GABA* (+ SR95531) was applied in the presence or absence of SKF89976A (20 μM).

(G) Normalized mean IPSC amplitude + SEM before (gray square) and after application of GABA (n = 7, green square), glutamate (n = 9, red square), glutamine (n = 12, blue square), GABA + SKF89976A (n = 6, green circle), and glutamate + TFB-TBOA (n = 5, red circle). Paired t test: ***p < 0.001, ** p < 0.01, * p < 0.05, n.s., not statistically significant.

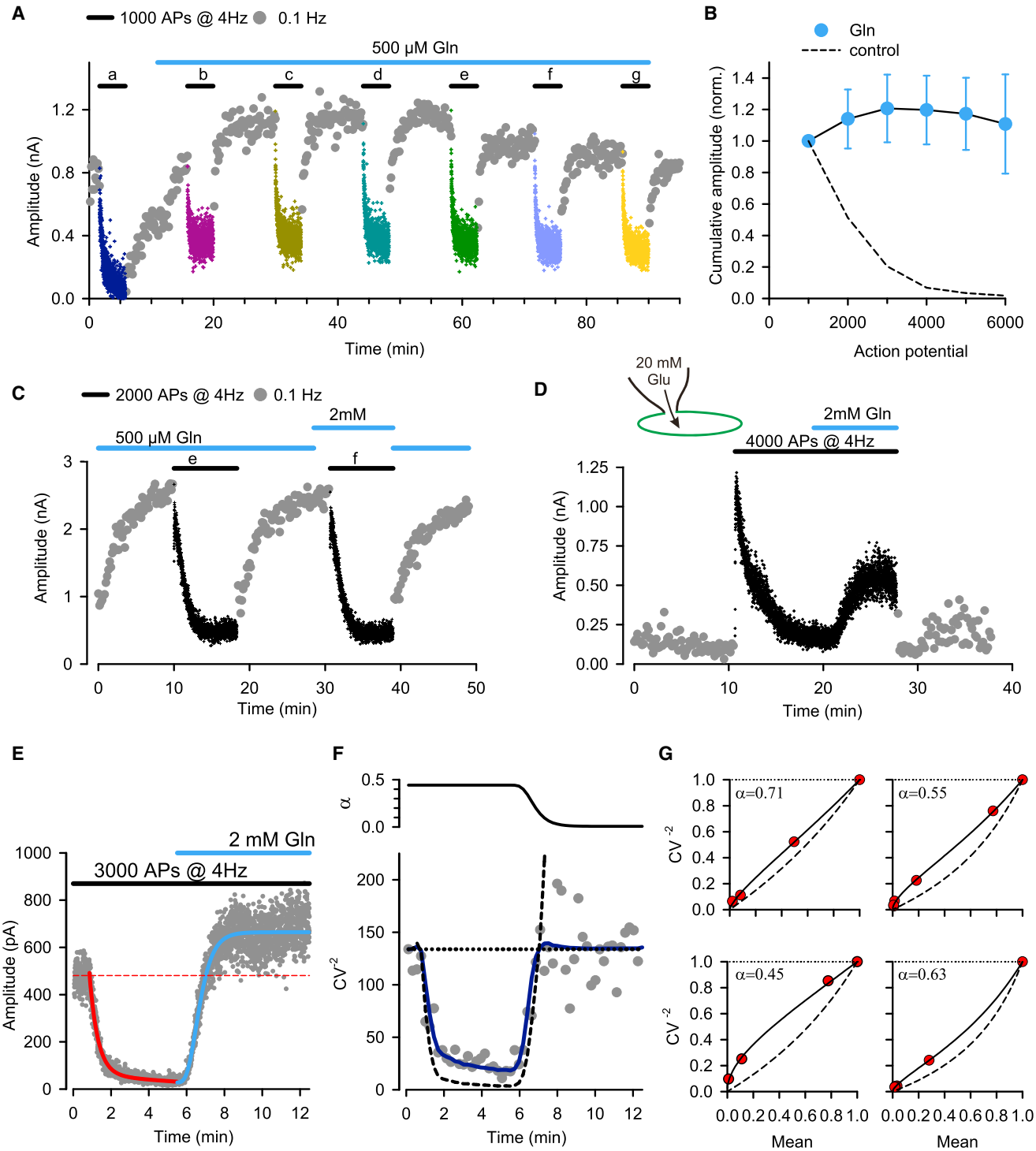

Figure 5. Glutamine Uptake Directly Supports GABA Filling of Recycling Vesicles

(A) Continuous application of glutamine (500 µM) maintains IPSC amplitude for multiple 4 Hz trains (a to g).

(B) Cumulative IPSC amplitude ± SEM for consecutive trains of APs in the continued presence of 500 µM glutamine (blue circles, n = 8) and in control neurons (dashed line, n = 21), normalized to the value of the first train.

(C) The steady IPSC amplitudes are similar during 4 Hz trains of 2,000 APs when glutamine is applied at 500 µM (train e) or 2 mM (train f).

(D) Time course of the IPSC amplitude evoked at 0.1 Hz (gray circles) and at 4 Hz (black crosses, solid line) in a facilitating pair. The presynaptic pipette contained 20 mM glutamate that maintained 28.7% of the initial cumulative amplitude after five trains of 2,000 APs (data not shown). Application of extracellular glutamine (2 mM, blue bar) potentiated GABA release.

(legend continued on next page)

associated with a faster time course of depression, could be explained if the number of recycling vesicles was dynamically controlled by the cytosolic GABA concentration.

GABA Depletion Reduced the Frequency of Miniature Asynchronous Release

To address this hypothesis, we recorded asynchronous miniature events to directly examine the quantal change during GABA depletion. Substitution of Sr^{2+} for Ca^{2+} in the extracellular solution reduced synchronous evoked IPSCs (eIPSCs) triggered at 1 Hz (Figure 7A, green trace). Evidence for asynchronous release in Sr^{2+} was indicated by a 2.2-fold increase in the frequency of miniature IPSCs (amIPSCs) detected over 200 ms after the stimulation (37.5 ± 4.0 Hz, n = 10; Figures 7A and 7B, red), compared to spontaneous miniature IPSCs (mIPSCs) measured before the AP (17.4 ± 2.1 Hz, n = 10, $p < 0.001$, Figures 7A and 7B, blue). On average, the amIPSCs frequency decayed to the mIPSCs frequency with a $\tau_w = 302 \pm 65$ ms (n = 8) and their initial mean amplitudes were not significantly different (amIPSC = 42 ± 6 pA and mIPSC = 29.7 ± 2.3 pA, respectively, n = 10, p = 0.24, Figure 7C).

Repetitive 1 Hz stimulation in Sr^{2+} induced a gradual rundown of the eIPSCs by 86.3% ± 2.5% after 3,000 APs (n = 10, $p < 0.001$, Figures 7D, 7E, and 7K). This rundown was associated with a 77.9% ± 7.7% reduction in amIPSC frequency (Figures 7F, 7H, 7J, and 7K; n = 10, $p < 0.001$) and a reduction in amIPSC amplitude of 33.3% ± 7% (n = 10, p = 0.007, Figures 7G, 7I, and 7K). Application of glutamine in a predepleted cell restored eIPSC to 45% of their initial amplitude (initial: 3,815 pA [data not shown]; depleted: 50 pA; restoration by glutamine: 1,700 pA; Figure 7L) and potentiated the frequency and amplitude of amIPSCs (Figures 7M and 7N). In four GABA-depleted pairs, the frequency of amIPSCs increased after glutamine application, from 15.2 ± 8.1 Hz to 41.3 ± 11.2 Hz (p = 0.026), whereas the frequency of mIPSCs remained unchanged (16.3 ± 9.3 Hz and 15.5 ± 8.2 Hz, p = 0.55). In addition, glutamine increased the amplitude of amIPSCs from 30.5 ± 4.2 pA to 47 ± 7.5 pA (p = 0.017) but not the amplitude of mIPSCs (34.3 ± 4.0 pA before and 37.7 ± 6.7 pA after glutamine uptake, p = 0.41).

The larger reduction in amIPSC frequency is in agreement with the hypothesis of a smaller pool of vesicles available for release as GABA is depleted.

Reduced Vesicles Cycling in Transmitter-Depleted Terminals

To directly examine vesicle recycling, we measured the labeling of synaptic vesicles in control (i.e., $[Gln]_e$ = 2 mM) and transmitter-depleted neurons with the fluorescent dye FM5-95 applied during the last train of the electrical field stimulation protocol (FM protocols are illustrated in Figure S6).

In contrast to the high-intensity fluorescence of FM5-95-stained puncta observed in control neurons (Figure 8A, left), we found that neurons incubated for 2 hr in a medium containing a reduced concentration of glutamine (20 μM) showed a significant reduction in FM5-95 labeling (Figure 8A, right). On average, the mean fluorescence intensity of FM5-95 spots decreased by 49%, from 2.8 ± 0.33 a.u. (n = 7) in control neurons to 1.47 ± 0.1 a.u. (n = 5, p = 0.005) in glutamine-depleted neurons (Figure 8B). The reduction in FM5-95 labeling indicated lower vesicle trafficking when transmitter supply was limiting for filling during a train of stimulation.

Next, we examined whether glutamine uptake restored vesicle cycling in transmitter-depleted neurons. Following electrical field stimulation that mimicked our depletion protocol in pairs (Figure S6), transmitter-depleted neurons were weakly stained with FM5-95 (Figure 8Ca). Repeating the electrical stimulation in the presence of glutamine (2 mM, see protocol in Figure S6) significantly increased the fluorescence intensity of FM5-95 puncta during a second FM application (Figures 8Cd and 8E). These results confirm that vesicle trafficking is regulated by the cytosolic transmitter concentration during sustained recycling activity.

FM-staining at EGFP-expressing varicosities was also specifically examined. A large fraction of these were colabeled by a fluorescent antibody against the C terminus of VIAAT (42% ± 1.7%; n = 3 experiments; Figure 8D). Comparison of the FM5-95 fluorescence in EGFP-varicosities and all puncta shows similar potentiation in the presence of glutamine, as shown in the inset of Figure 8E, although the absolute fluorescence was lower at EGFP-expressing varicosities (Figure 8C).

Together, these results confirm that cycling vesicle trafficking was reduced as cytosolic transmitter is depleted, a mechanism that preserves GABA resource and a threshold amount of GABA in released vesicles.

DISCUSSION

The availability of release-ready vesicles is considered the limiting factor in sustaining Ca^{2+}-evoked exocytosis at small central synapses (Neher, 2010; Zucker and Regehr, 2002), although maintaining transmission obviously requires that vesicles be filled with neurotransmitter before release (for review see Südhof, 2004). At inhibitory synapses, the VIAAT-mediated loading process remains poorly characterized, despite evidence indicating that alterations in GABA release are a presynaptic source of variability and plasticity (Barberis et al., 2004; Engel et al., 2001; Frerking et al., 1995).

(E) Time course of IPSC amplitude evoked at 4 Hz for 3,000 APs in a prestimulated neuron (5,000 APs, data not shown). Application of glutamine (2 mM, blue bar) restored GABA release. The red dashed line is the mean amplitude at the onset of the train. The solid red line is a biexponential fit with $\tau_1 = 26.4$ s and $\tau_2 = 376$ s. The solid blue line is the fit with a modified Gompertz equation with $\tau = 29$ s.

(F) CV^{-2} plotted as function of time for the experiment shown in (E). The lines are the predicted CV^{-2} for a pure change in q (dotted line), pure change in p (dashed line), and mixed change (blue solid line). Top panel represents α, the relative fraction for the change in p ($p = x^{\alpha}$ and $q = x^{(1-\alpha)}$, where x is the normalized amplitude).

(G) CV^{-2}-mean relationship for four representative pairs. The mean amplitude and CV^{-2} were calculated for the last 270 APs of each train and normalized by the initial value. The lines are the predicted CV^{-2} for a binomial equation assuming pure change in q (dot line), pure change in p (dashed line), or mixed change (solid line). The α value is indicated for each pair, see also Figure S5.

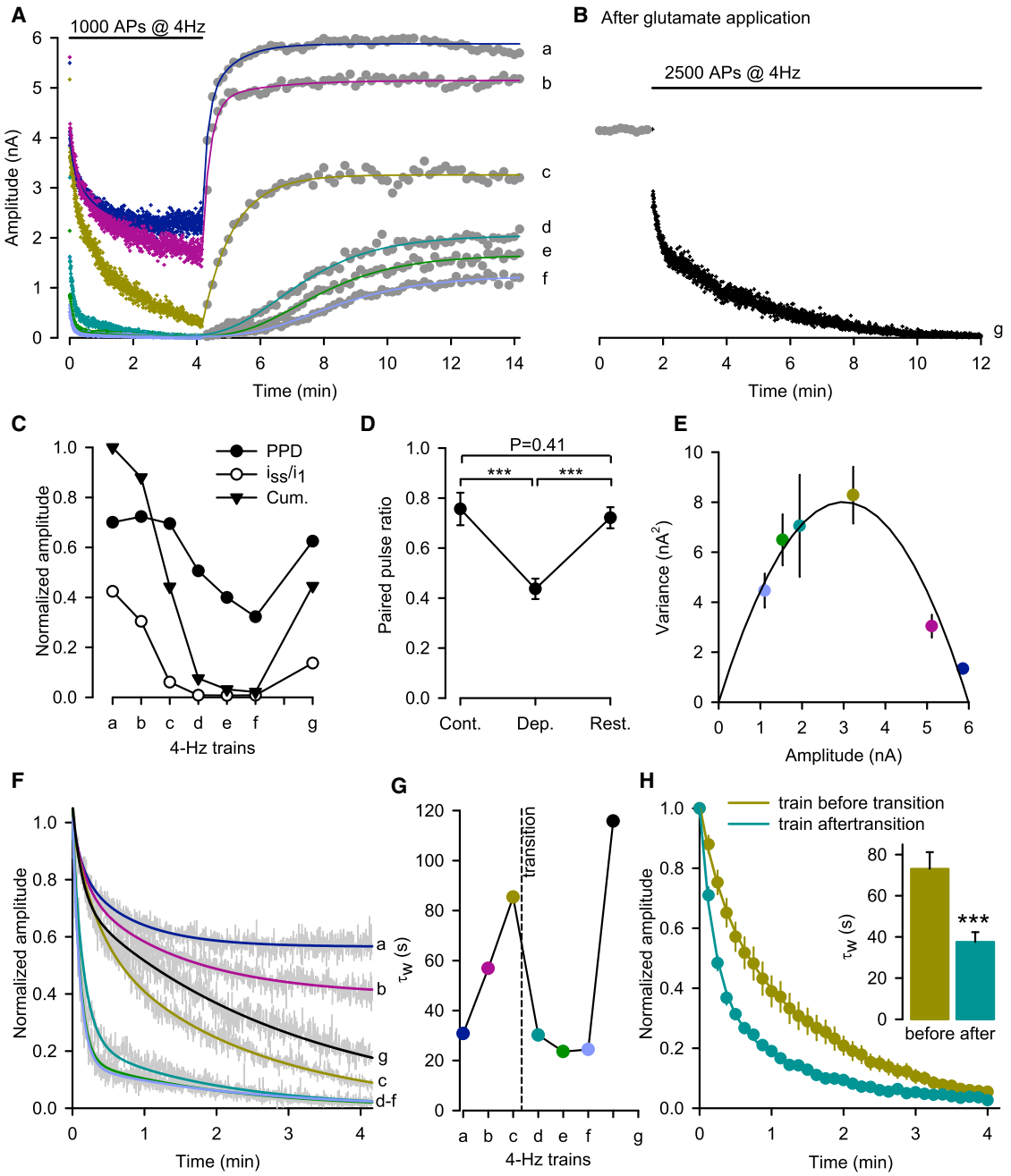

Figure 6. GABA Depletion Decreases the Release Probability

(A) Change in the time course of depression during six (a to f) consecutive 4 Hz trains of 1,000 APs (colored crosses) and recovery (0.1 Hz, gray circles) in a high-releasing cell. The solid lines represent exponential fits to the data at 0.1 Hz.

(B) Collapse of transmission within 2,500 APs at 4 Hz after recovery by glutamate application (50 μM, data not shown) for the (same cell as in A).

(C) Paired-pulse depression (closed circles) at onset of 4 Hz train, average steady-state amplitude (open circles) for the last 30 APs of each train normalized to the initial amplitude and cumulative amplitude (closed triangles) for each 4 Hz train normalized by the first value.

(D) Average ± SEM paired-pulse depression in control (cont), after GABA depletion (dep), and restoration of GABA supply (rest) for nine pairs with high releasing properties. Paired t test.

(E) Variance ± SEM mean amplitude plot for the recovery at 0.1 Hz after each train as indicated by the same color code as in (A). The solid line represents the fit for a simple binomial model with pure change in p.

(F) Biexponential fit of the time course of depression for the six 4 Hz trains shown in (A). The first IPSC was disregarded.

(G) Weighted time constants for each train shown in (F).

(H) Average ± SEM time course of depression for trains evoked before and after the kinetic transition induced by GABA depletion in nine pairs. The solid line represents biexponential fits. Inset: average + SEM weighted time constants for the train before and after the transition. Paired t test.

Somatic GABA Supply Partially Supports VIAAT Loading at Presynaptic Terminals

We show that sustained vesicle recycling together with whole-cell dialysis can exhaust all cytosolic sources of GABA when neurons have access only to D-glucose, as neurons cannot synthesize GABA from D-glucose (Bak et al., 2006). This starvation condition is opposite to the ad libitum access to glutamine prevailing in culture media (2 mM) or in vivo (~0.5 mM). Although soluble cytosolic factors may have been diluted by prolonged whole-cell recordings—e.g., GABA stocks, factors involved in the vesicle cycle (Ertunc et al., 2007; Kraushaar and Jonas, 2000), or GABA synthesis—we showed that the GABA depletion described here originates mainly from an activity-dependent consumption of the cytosolic stocks of GABA and its precursors. This transmitter depletion suggests that the amount of GABA needed to fill the pool of recycling vesicles is not negligible, as expected if VIAAT operates near its thermodynamic equilibrium (1,000-fold accumulation for 1 H^+/1 GABA stoichiometry; see Edwards, 2007).

High concentrations (10–20 mM) of GABA or glutamate in the presynaptic pipette partially prevented rundown of transmission, indicating that diffusion from the cell body can supply GABA to fast recycling vesicle, as shown for glycine at spinal cord and brainstem synapses (Apostolides and Trussell, 2013; Rousseau et al., 2008).

GABA Availability Regulates the Vesicle Cycle

It is generally accepted that the vesicle and the transmitter cycles are not directly coupled (Edwards, 2007) because empty vesicles can undergo futile cycles of exo-/endocytosis (Croft et al., 2005; Hori and Takahashi, 2012; Parsons et al., 1999; Tabares et al., 2001; Wojcik et al., 2004; Zhou et al., 2000).

However, our data suggest that the accumulation of empty vesicles in GABA-depleted synapses during long episodes of stimulation somehow slows their reuse. Quantal analysis of amIPSCs recorded in Sr^{2+} during GABA depletion shows that their mean amplitude was maintained well above detection threshold, suggesting that vesicles released an amount of GABA that is equal to or greater than some minimum. Furthermore, the reduction in amIPSC frequency and the reduction in release probability suggest that GABA depletion decreased the number of quanta released, as observed in choline-deprived *Aplysia* neurons (Poulain et al., 1986) and consistent with the reduction in frequency of miniature and spontaneous IPSCs produced by inhibition of GABA synthesis (Engel et al., 2001; Obata et al., 2008).

Our results confirm that rapid filling of recycling vesicles maintains the plateau phase of GABA release during repeated stimulation (Ertunc et al., 2007; Kraushaar and Jonas, 2000). Manipulations that compromise vesicle filling either by reducing vesicle reacidification (Ertunc et al., 2007) or, as shown here, by depleting cytosolic GABA increase the extent but also the rate of synaptic depression, suggesting a reduction of the pool of vesicles available for release. In contrast, increasing the luminal pH buffer of recycling vesicles generated by miniature IPSCs was found to reduce their amplitude but not their frequency (Riazanski et al., 2011). These differences argue for an activity-dependent regulation in the trafficking of empty vesicles. In agreement, we show a significant reduction in FM5-95 vesicle labeling in glutamine-depleted neurons that is restored by resupplying glutamine.

Reversible reduction of the pool of releasable vesicles may preserve their filling under limited GABA resources. Recent evidence supports the existence of dynamic exchanges between pools of cycling and resting vesicles at small central synapses (see review in Denker and Rizzoli, 2010), for example by regulating the balance of CDK5/calcineurin activity (Kim and Ryan, 2010; Marra et al., 2012).

Critical Roles of Neuronal Transporters for Presynaptic GABA Supply

After activity-dependent rundown, inhibitory transmission was restored in minutes by initiating GABA, glutamate, or glutamine uptake. This clearly demonstrates that presynaptic vesicle cycling and GABA synthesis remain functional during the rundown and is in agreement with anatomical evidence indicating that GAT1 (Chiu et al., 2002; Fish et al., 2011), EAAC1 (Conti et al., 1998; He et al., 2000), and SNAT1/SAT1 (Solbu et al., 2010) are expressed in the axon and terminals of GABAergic neurons.

In contrast to the critical role of the neuronal glycine transporter GlyT2 in glycinergic transmission (Apostolides and Trussell, 2013; Gomeza et al., 2003; Rousseau et al., 2008), genetic inactivation and pharmacological inhibition of GAT1, EAAC1, or SNAT1/SAT1 show that none of these transporters is essential for vesicular GABA release. Although GAT1 is responsible for 95% GABA uptake in synaptosomes (Chiu et al., 2002), its inactivation in $GAT1^{-/-}$ knockout mice increased extracellular GABA without disrupting transmission or GABA accumulation in terminals (Bragina et al., 2008; Chiu et al., 2005; Jensen et al., 2003) and the behavioral defects phenocopy the clinical side effects of Tiagabine, an antiepileptic GAT1 inhibitor (Chiu et al., 2005). Inhibition of EAAC1 decreased the amplitude of miniature and spontaneous IPSCs in hippocampal slices (Mathews and Diamond, 2003; Sepkuty et al., 2002) and EAAC1 knockdown induces seizures indicating excitation/inhibition imbalance (Rothstein et al., 1996; Sepkuty et al., 2002).

Our results show that GABAergic neurons grown in media containing glutamine have the capacity to maintain significant cytosolic GABA stores and continue to fill vesicles during the prolonged absence of extracellular glutamine. A similar reservoir was also demonstrated for glutamate in excitatory hippocampal neurons (Kam and Nicoll, 2007), indicating that it may be a common feature to glutamine-supplied neurons. This cytosolic GABA stock and the activity- and age-dependent change in SNAT1/SAT1 expression (Brown and Mathews, 2010) makes it difficult to dissect the contribution of the glutamate/glutamine cycle for GABA vesicular release. Nevertheless previous work has shown that blocking neuronal glutamine uptake or astrocytic glutamine synthesis decreased the amplitude of evoked and miniature GABAergic IPSCs in hippocampal slices (Fricke et al., 2007).

In conclusion, our data show the synergy between GABA, glutamate, and glutamine transporters and VIAAT-mediated vesicular accumulation of GABA. In addition, our results suggest that the vesicle cycle adapts to prolonged GABA depletion by reducing the number of recycling vesicles, thus matching available GABA resources.

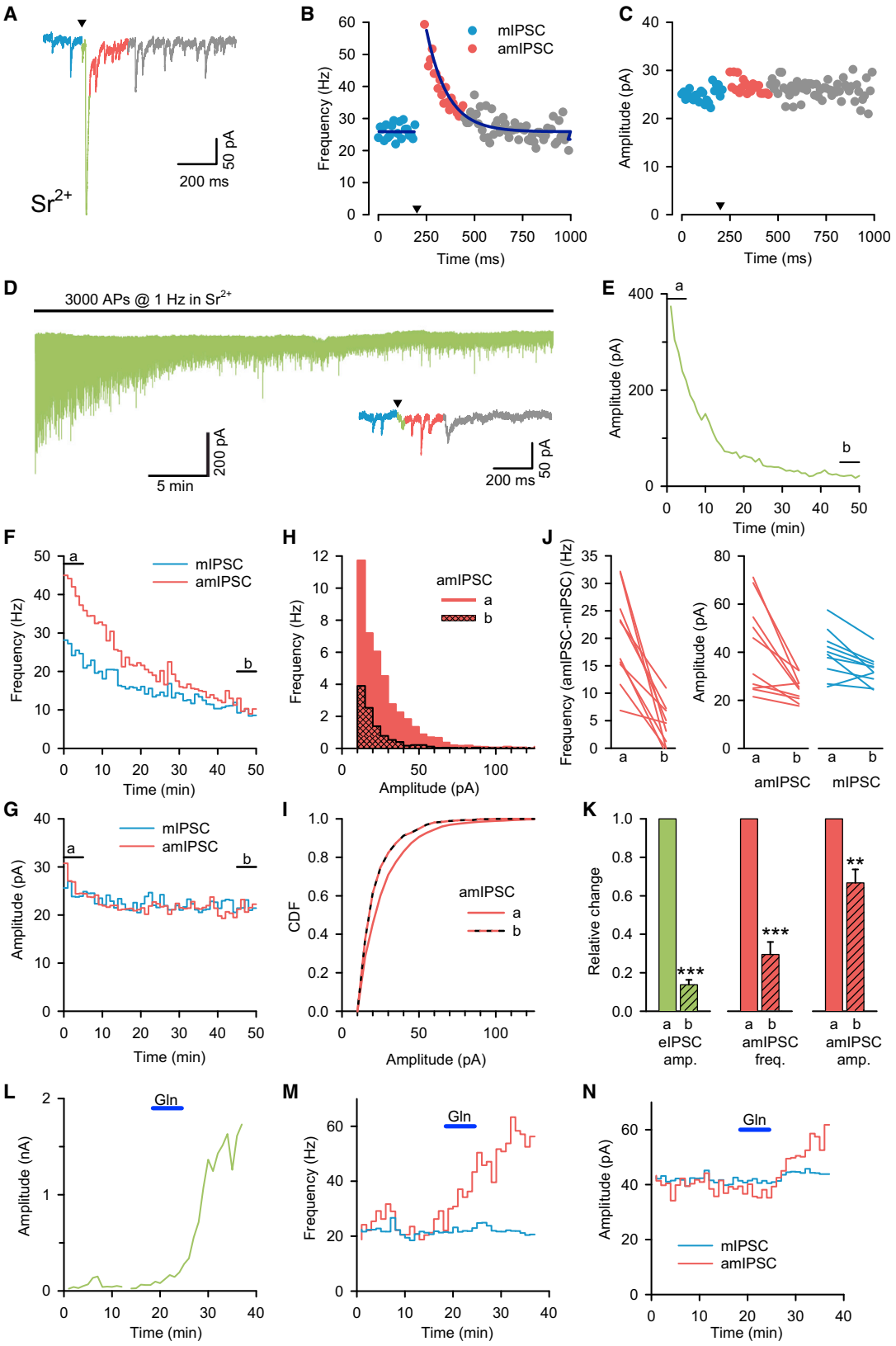

(legend on next page)

EXPERIMENTAL PROCEDURES

Primary Neuron Cultures

Neonatal hippocampal neurons derived from heterozygous transgenic mice from the GAD65_3e/gfp5.5#30 line (López-Bendito et al., 2004) on a C57BL/6 background were cultured on an astroglial monolayer as described in (Kaech and Banker, 2006) (for more details, see Supplemental Experimental Procedures).

Electrophysiology

Paired whole-cell patch-clamp recordings of identified inhibitory connections were performed at ~30°C in cultured hippocampal neurons (8–20 days in vitro). Neurons were continuously bathed with an external solution containing 140 mM NaCl, 2.4 mM KCl, 2 mM $CaCl_2$, 1 mM $MgCl_2$, 10 mM glucose, and 10 mM HEPES (pH 7.4). The internal solution for presynaptic neurons contained 155 mM K-gluconate, 4 mM KCl, 0.1 mM EGTA, 5 mM Mg-ATP, 0.2 mM Pyridoxal 5′-phosphate, and 10 mM HEPES adjusted to pH 7.4 with KOH. The internal solution for the postsynaptic cells contained 140 mM CsCl, 1 mM $CaCl_2$, 1 mM $MgCl_2$, 10 mM EGTA, 1 mM BAPTA, 5 mM Mg-ATP, 5 mM QX314, and 10 mM HEPES, adjusted to pH 7.4 with CsOH. The osmolarities of all solutions were 290–300 mOsm (for more details, see Supplemental Experimental Procedures).

Asynchronous Events

Sr^{2+} was substituted for Ca^{2+} in the external solution to record miniature-like asynchronous events at 0.1 or 1 Hz. Data were analyzed offline using SpAcAn (http://www.spacan.net). Synchronous synaptic responses were detected during the 10 ms period after the peak of AP. Miniature events were detected during the 10 s or 1 s sweeps starting 20 ms after the peak of AP. The threshold was set at 10 pA in most recordings.

Data Analysis

The latency for paired recordings corresponds to the delay between the peak of the action potential and the maximum of the rising slope of the IPSC. The IPSC peak amplitudes are plotted as absolute values in time course plot. The IPSC decay was fitted by the sum of two exponentials: $A_t = A_1\, e^{-(t-t_0)/\tau_1} + A_2\, e^{-(t-t_0)/\tau_2}$, where A_1 and A_2 are the amplitudes of the two components and τ_1 and τ_2 are the time constants. The amplitude-weighted decay time constant is calculated as: $\tau_w = (A_1\,\tau_1 + A_2\,\tau_2)/A_1 + A_2$.

The time course for short-term depression was fitted by a sum of exponentials (typically 2) with an offset. The first IPSC in a train was not included because of its undefined frequency. Recovery at 0.1 Hz was fitted with mono- or biexponential time course:

$$A_t = A_0 + A_1\left(1 - e^{-(t-t_0)/\tau_1}\right) + A_2\left(1 - e^{-(t-t_0)/\tau_2}\right),$$

while sigmoid time courses were best fitted using a modified Gombertz equation:

$$A_t = A_0 + A_1 e^{-e^{-(t-t_0)/\tau}}.$$

The cumulative amplitude represents the sum of the peak absolute amplitudes of the IPSC evoked during a 4 Hz train. The cumulative IPSC amplitude for the i_{th} train is indicated as Cumulative $Amplitude_i$.

Segmented variance was calculated for multiple of three IPSCs with no overlap. The normalized changes in CV^{-2} and variance were fitted as function of time (Figure 5F) or mean amplitude (Figures 5G and 6E) using the set of equations for a simple binomial model:

$$\begin{cases} x = \dfrac{A}{n\,p\,q} \\ VAR = n\,p\,q^2 x^{(2-\alpha)}(1 - p\,x^{\alpha}) \\ CV^{-2} = \dfrac{n\,p\,x^{\alpha}}{1 - p\,x^{\alpha}} \end{cases}$$

where n is the apparent number of release sites, p is the apparent release probability, and q is the apparent quantal size; x corresponds to the amplitude change, with a fraction x^{α} for p change and $x^{(1\,-\,\alpha)}$ for q change (Kraushaar and Jonas, 2000).

FM-Based imaging

Recycling synaptic vesicles were labeled with the styryl dye FM5-95 (Molecular Probes) during a single train of field stimulation using a pair of platinum wires placed across a 12 mm coverslip (biphasic current pulses of 10 mA using an A-M system 2100 stimulator). Stimulation protocols consisting of cycles of 1,000 pulses at 4 Hz and 60 pulses at 0.1 Hz, similar to those used to induce "rundown" in the electrophysiological experiments, were controlled and chained by PClamp 8 using a Digidata 1200 interfaced with the stimulator. The external solution contained NBQX (5 μM), MK801 (2 μM), 5,7-Dichlorokynurenic acid (5 μM), and SR95531 (5 μM) to prevent recurrent activity. All experiments were performed at 28°C–30°C, and FM5-95 (5 μM) was added during the final train of stimulation. Surface FM labeling was washed off for 15 min with control solution + ADVASEP-7 (1 mM) before imaging (see Figure S6).

We used two protocols for depleting the cytosolic stocks of glutamate and GABA, as shown in Figure S6. First, the glutamine concentration in the growth media was decreased from 2 mM (control) to 20 μM (glutamine depleted) 2 hr before electrical field stimulation. Alternatively, the coverslip was stimulated electrically by seven cycles in the absence of external glutamine and the presence of glutamate and GABA receptor inhibitors. FM5-95 was added only during the seventh train. After image acquisition, electrical stimulation was reinstated for one to three trains. Glutamine (2 mM) was applied for 10 min and a second FM application was carried out during the last train (Figure S6).

Identification of inhibitory synapses at EGFP boutons was carried out using the VIAAT antibody against the C-term luminal domain, fluorescence labeled with Oyster-650 (Synaptic System). Although sparse labeling with VIAAT

Figure 7. Quantal Changes Underlying GABA-Dependent Transmission Collapse and Restoration

(A) Representative 1 s sweep recorded in Sr^{2+} at the onset of the 1 Hz stimulation shown in (D). A significant evoked IPSC (eIPSC) component was still detectable within a time window of 10 ms after APs (green trace), whereas numerous asynchronous miniature-like IPSCs (amIPSCs, red trace) were detected within a time window of 200 ms following the AP. mIPSCs were analyzed in a 200 ms time window (blue trace) before AP (black triangle).

(B) Average frequency of mIPSCs (blue) and amIPSCs (red) detected every 20 ms during 1 s sweep for the first 300 APs. The solid line represents the exponential fit, with a time constant of 110 ms.

(C) Average amplitude of mIPSCs (blue) and amIPSCs (red) detected as in (B).

(D) Trace of eIPSCs during continuous stimulation (3,000 APs at 1 Hz) in the presence of Sr^{2+}. Inset: representative 1 s sweep at the end of the recording.

(E) Time course of the eIPSC amplitude at 1 Hz in presence of 2 mM Sr^{2+}.

(F and G) Frequency (F) and amplitude (G) of mIPSCs (blue line) and amIPSCs (red line) recorded in the same experiment as in (E).

(H and I) Frequency (H) and cumulative distribution function of the amplitude (I) for amIPSCs during 300 sweeps at onset (a, red) and end (b, red dashed).

(J) Change in frequency (left) and amplitude (right) for the mIPSCs (blue) and amIPSC (red) recorded at onset (a) and end (b) of the 1 Hz stimulation for ten pairs.

(K) Bar graph of the relative change + SEM of eIPSC amplitude (green) and amIPSC amplitude and frequency (red) at onset (a, solid) and end (b, dash) of the 1 Hz stimulation; paired t test.

(L) Glutamine (2 mM, blue bar) restored the amplitude of eIPSC at 0.1 Hz in a GABA predepleted neuron previously stimulated with 7,000 APs (data not shown; $eIPSC_{depleted}/eIPSC_{initial}$ = 0.013).

(M and N) Frequency (M) and amplitude (N) of amIPSCs during restoration by glutamine.

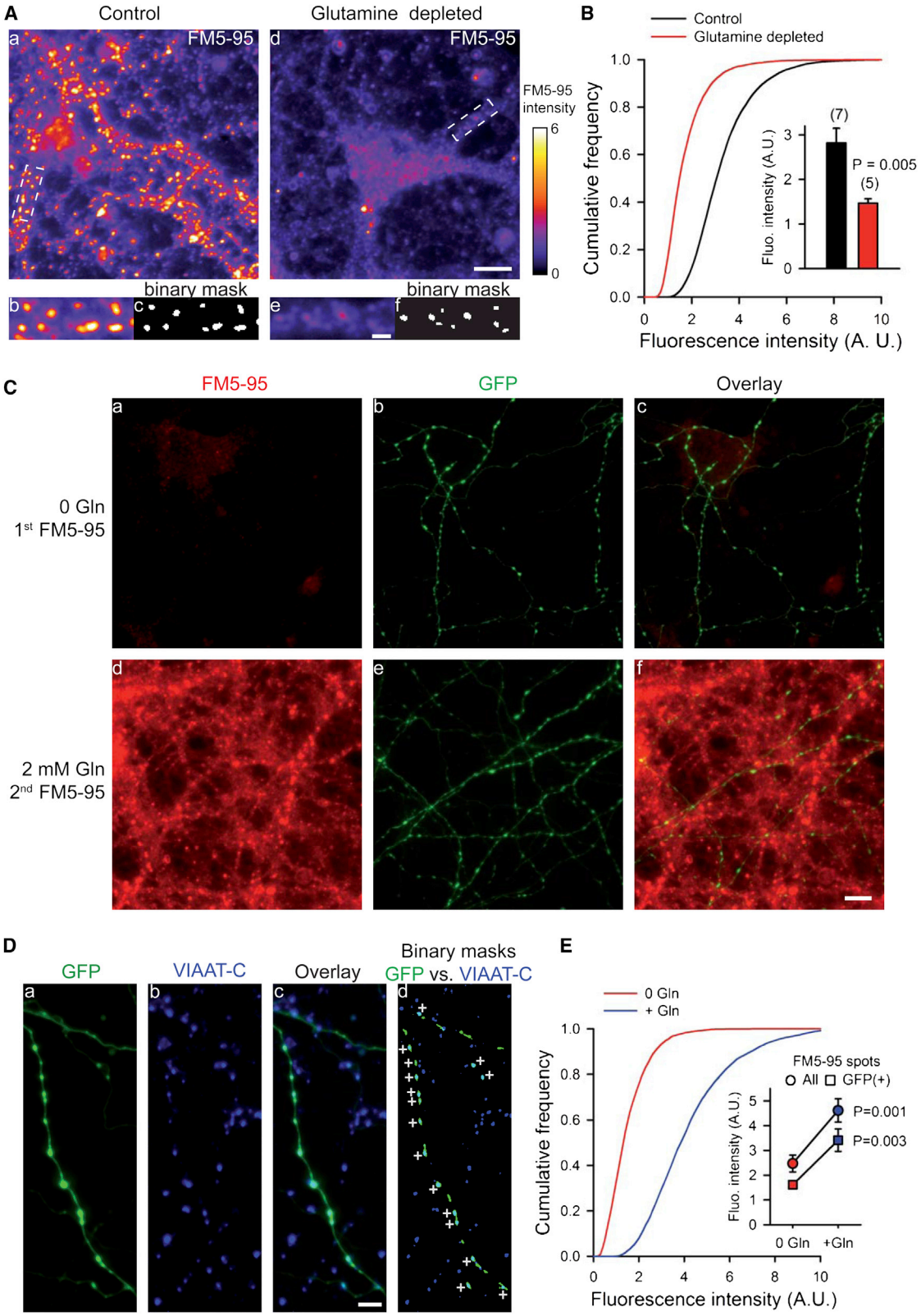

(legend on next page)

antibody could be observed after one train of electrical field stimulation, more robust staining was obtained during prolonged incubation with the antibody (2–12 hr; 0.5 μg/coverslip). We found that 13% ± 1.2% (n = 3) of VIAAT(+)-labeled spots were EGFP(+), in agreement with EGFP being expressed in transgenic GAD65:EGFP mice only in a subset of interneurons derived from the caudal-ganglionic eminence (López-Bendito et al., 2004; Tricoire et al., 2011).

Fluorescence images of FM5-95, EGFP, and Oyster-650 were acquired on an Olympus IX71 microscope using a 60× LUCPLFLN 0.7 NA objective and a high-illumination light source (SOLA Lumencor). Images of 1,002 × 1,004 pixels were collected using an iXON 885 ANDOR camera controlled by micromanager (NIH). During image acquisition, Mg^{2+} replaced Ca^{2+} in the external solution to reduce Ca^{2+} dependent exocytosis.

Ten images were typically acquired for each condition and the quantification of fluorescence was carried out on raw images using ICY (de Chaumont et al., 2012). Binary images of FM5-95 and EGFP puncta were generated using the ICY spot detector plugin (Olivo-Marin, 2002), and FM5-95 fluorescence intensities are the average intensity of individual spots, with an average density of 4 ± 0.2 FM spots/100 μm^2 (n = 15 experiments). Images were processed using ImageJ (NIH). Panel D in Figure 8 was filtered using ICY median filter (half size of 2).

Statistics

Results are reported as mean ± SEM with the sample size indicated in parentheses. Student's t test or Mann-Whitney rank-sum test was used to assess differences between two related or independent sample groups using SigmaPlot software. Asterisks indicate *$p < 0.05$, **$p < 0.01$, and ***$p < 0.001$. n.s. signifies no statistical difference.

SUPPLEMENTAL INFORMATION

Supplemental Information includes Supplemental Experimental Procedures and six figures and can be found with this article online at http://dx.doi.org/10.1016/j.neuron.2013.07.021.

ACKNOWLEDGMENTS

We thank Gábor Szabó for the generous gift of the EGFP-GAD65 mice. We thank Boris Barbour, Philippe Ascher, and Mariano Casado for critical reading and suggestions; Stéphane Dieudonné, Païkan Marcaggi, and Bernard Poulain for stimulating discussions; Guillaume Dugué and Charly Rousseau for SpAcAn development; and Pr Yinghe Hu for his interest. This project is supported by the CNRS, INSERM, and a grant from the Association Française contre les Myopathies (AFM). L.W. was supported by fellowships from East China Normal University, the CHINA Scholarship Council, the Fondation pour la Recherche Médicale, and a grant from the Region Ile de France. P.T. was supported by postdoctoral fellowships from the Neuroscience pole of Research in Ile de France (NeRF) and the Fondation Pierre-Gilles de Gennes. L.B. is a recipient of Ministère de la Recherche et de la Technologie PhD fellowship. K.A. was supported by a postdoctoral fellowship from the Association Française contre les Myopathies (AFM).

Accepted: July 19, 2013
Published: October 2, 2013

REFERENCES

Apostolides, P.F., and Trussell, L.O. (2013). Rapid, activity-independent turnover of vesicular transmitter content at a mixed glycine/GABA synapse. J. Neurosci. *33*, 4768–4781.

Asada, H., Kawamura, Y., Maruyama, K., Kume, H., Ding, R.G., Kanbara, N., Kuzume, H., Sanbo, M., Yagi, T., and Obata, K. (1997). Cleft palate and decreased brain gamma-aminobutyric acid in mice lacking the 67-kDa isoform of glutamic acid decarboxylase. Proc. Natl. Acad. Sci. USA *94*, 6496–6499.

Atluri, P.P., and Ryan, T.A. (2006). The kinetics of synaptic vesicle reacidification at hippocampal nerve terminals. J. Neurosci. *26*, 2313–2320.

Aubrey, K.R., Rossi, F.M., Ruivo, R., Alboni, S., Bellenchi, G.C., Le Goff, A., Gasnier, B., and Supplisson, S. (2007). The transporters GlyT2 and VIAAT cooperate to determine the vesicular glycinergic phenotype. J. Neurosci. *27*, 6273–6281.

Bak, L.K., Schousboe, A., and Waagepetersen, H.S. (2006). The glutamate/GABA-glutamine cycle: aspects of transport, neurotransmitter homeostasis and ammonia transfer. J. Neurochem. *98*, 641–653.

Barberis, A., Petrini, E.M., and Cherubini, E. (2004). Presynaptic source of quantal size variability at GABAergic synapses in rat hippocampal neurons in culture. Eur. J. Neurosci. *20*, 1803–1810.

Bragina, L., Marchionni, I., Omrani, A., Cozzi, A., Pellegrini-Giampietro, D.E., Cherubini, E., and Conti, F. (2008). GAT-1 regulates both tonic and phasic GABA(A) receptor-mediated inhibition in the cerebral cortex. J. Neurochem. *105*, 1781–1793.

Brown, M.N., and Mathews, G.C. (2010). Activity- and age-dependent modulation of GABAergic neurotransmission by system A-mediated glutamine uptake. J. Neurochem. *114*, 909–920.

Chiu, C.S., Jensen, K., Sokolova, I., Wang, D., Li, M., Deshpande, P., Davidson, N., Mody, I., Quick, M.W., Quake, S.R., and Lester, H.A. (2002). Number, density, and surface/cytoplasmic distribution of GABA transporters at presynaptic structures of knock-in mice carrying GABA transporter subtype 1-green fluorescent protein fusions. J. Neurosci. *22*, 10251–10266.

Chiu, C.S., Brickley, S., Jensen, K., Southwell, A., Mckinney, S., Cull-Candy, S., Mody, I., and Lester, H.A. (2005). GABA transporter deficiency causes tremor, ataxia, nervousness, and increased GABA-induced tonic conductance in cerebellum. J. Neurosci. *25*, 3234–3245.

Conti, F., DeBiasi, S., Minelli, A., Rothstein, J.D., and Melone, M. (1998). EAAC1, a high-affinity glutamate tranporter, is localized to astrocytes and gabaergic neurons besides pyramidal cells in the rat cerebral cortex. Cereb. Cortex *8*, 108–116.

Croft, B.G., Fortin, G.D., Corera, A.T., Edwards, R.H., Beaudet, A., Trudeau, L.E., and Fon, E.A. (2005). Normal biogenesis and cycling of empty synaptic vesicles in dopamine neurons of vesicular monoamine transporter 2 knockout mice. Mol. Biol. Cell *16*, 306–315.

Figure 8. FM5-95 Uptake Is Reversibly Reduced in GABA-Depleted Neurons

(A) Top: images of FM5-95 staining in (a) control neurons with unrestrained access to glutamine and (d) neurons maintained for 2 hr with 20 μM glutamine (see protocol in Figure S6). The bottom panels show (b and e) enlargements of the dashed boxes shown in (a) and (d), together with (c and f) the ICY binary masks for the detected FM5-95 spots. The scale bar represents 10 μm in (d) and 2 μm in (e).

(B) Cumulative frequency of FM5-95 fluorescence intensity in control neurons (black line, 1,251 ± 64 spots/image, nine images) and glutamine-depleted neurons (red line, 986 ± 15 spots/image, eight images, p = 0.002) for the experiment shown in (A). Inset: mean + SEM fluorescence intensity for control neurons (black, n = 7 experiments) and glutamine-depleted neurons (red, n = 5 experiments, p = 0.005, t test).

(C) Images of FM5-95 staining (a and d), EGFP (b and e), and overlay (c and f) following depletion induced by seven trains of 1,000 stimulations at 4 Hz (a, b, and c) and after 10 min glutamine application (d, e, and f) (same coverslip and intensity scale; see protocol in Figure S6).

(D) EGFP(+) varicosities express VIAAT: EGFP varicosities (a), VIAAT C-luminal antibody (b), overlay (c), and binary masks overlay (d) of ICY-detected VIAAT spots (blue) and EGFP spots (green). The plus signs indicate colocalized VIAAT and EGFP spots.

(E) Cumulative frequency of the fluorescence intensity detected at FM5-95 spots in transmitter-depleted neurons (red line, 717 ± 75 puncta/image, n = 6 experiments) and after glutamine application (blue line; 755 ± 83 puncta/image, p = 0.69). Inset: mean + SEM fluorescence intensity in transmitter-depleted neurons (red) and after application of glutamine (blue) for all puncta (circles, n = 7) and EGFP(+) puncta only (squares, n = 7). Paired t test.

de Chaumont, F., Dallongeville, S., Chenouard, N., Hervé, N., Pop, S., Provoost, T., Meas-Yedid, V., Pankajakshan, P., Lecomte, T., Le Montagner, Y., et al. (2012). Icy: an open bioimage informatics platform for extended reproducible research. Nat. Methods *9*, 690–696.

Denker, A., and Rizzoli, S.O. (2010). Synaptic vesicle pools: an update. Front. Synaptic Neurosci. *2*, 135.

Edwards, R.H. (2007). The neurotransmitter cycle and quantal size. Neuron *55*, 835–858.

Engel, D., Pahner, I., Schulze, K., Frahm, C., Jarry, H., Ahnert-Hilger, G., and Draguhn, A. (2001). Plasticity of rat central inhibitory synapses through GABA metabolism. J. Physiol. *535*, 473–482.

Ertunc, M., Sara, Y., Chung, C., Atasoy, D., Virmani, T., and Kavalali, E.T. (2007). Fast synaptic vesicle reuse slows the rate of synaptic depression in the CA1 region of hippocampus. J. Neurosci. *27*, 341–354.

Fish, K.N., Sweet, R.A., and Lewis, D.A. (2011). Differential distribution of proteins regulating GABA synthesis and reuptake in axon boutons of subpopulations of cortical interneurons. Cereb. Cortex *21*, 2450–2460.

Frerking, M., Borges, S., and Wilson, M. (1995). Variation in GABA mini amplitude is the consequence of variation in transmitter concentration. Neuron *15*, 885–895.

Fricke, M.N., Jones-Davis, D.M., and Mathews, G.C. (2007). Glutamine uptake by System A transporters maintains neurotransmitter GABA synthesis and inhibitory synaptic transmission. J. Neurochem. *102*, 1895–1904.

Gomeza, J., Hülsmann, S., Ohno, K., Eulenburg, V., Szöke, K., Richter, D., and Betz, H. (2003). Inactivation of the glycine transporter 1 gene discloses vital role of glial glycine uptake in glycinergic inhibition. Neuron *40*, 785–796.

He, Y., Janssen, W.G., Rothstein, J.D., and Morrison, J.H. (2000). Differential synaptic localization of the glutamate transporter EAAC1 and glutamate receptor subunit GluR2 in the rat hippocampus. J. Comp. Neurol. *418*, 255–269.

Hori, T., and Takahashi, T. (2012). Kinetics of synaptic vesicle refilling with neurotransmitter glutamate. Neuron *76*, 511–517.

Jensen, K., Chiu, C.S., Sokolova, I., Lester, H.A., and Mody, I. (2003). GABA transporter-1 (GAT1)-deficient mice: differential tonic activation of GABAA versus GABAB receptors in the hippocampus. J. Neurophysiol. *90*, 2690–2701.

Kaech, S., and Banker, G. (2006). Culturing hippocampal neurons. Nat. Protoc. *1*, 2406–2415.

Kam, K., and Nicoll, R. (2007). Excitatory synaptic transmission persists independently of the glutamate-glutamine cycle. J. Neurosci. *27*, 9192–9200.

Kavalali, E.T. (2006). Synaptic vesicle reuse and its implications. Neuroscientist *12*, 57–66.

Kim, S.H., and Ryan, T.A. (2010). CDK5 serves as a major control point in neurotransmitter release. Neuron *67*, 797–809.

Klausberger, T., Magill, P.J., Márton, L.F., Roberts, J.D., Cobden, P.M., Buzsáki, G., and Somogyi, P. (2003). Brain-state- and cell-type-specific firing of hippocampal interneurons in vivo. Nature *421*, 844–848.

Kraushaar, U., and Jonas, P. (2000). Efficacy and stability of quantal GABA release at a hippocampal interneuron-principal neuron synapse. J. Neurosci. *20*, 5594–5607.

López-Bendito, G., Sturgess, K., Erdélyi, F., Szabó, G., Molnár, Z., and Paulsen, O. (2004). Preferential origin and layer destination of GAD65-GFP cortical interneurons. Cereb. Cortex *14*, 1122–1133.

Marra, V., Burden, J.J., Thorpe, J.R., Smith, I.T., Smith, S.L., Häusser, M., Branco, T., and Staras, K. (2012). A preferentially segregated recycling vesicle pool of limited size supports neurotransmission in native central synapses. Neuron *76*, 579–589.

Mathews, G.C., and Diamond, J.S. (2003). Neuronal glutamate uptake Contributes to GABA synthesis and inhibitory synaptic strength. J. Neurosci. *23*, 2040–2048.

Neher, E. (2010). What is rate-limiting during sustained synaptic activity: vesicle supply or the availability of release sites. Front. Synaptic Neurosci. *2*, 144.

Obata, K., Hirono, M., Kume, N., Kawaguchi, Y., Itohara, S., and Yanagawa, Y. (2008). GABA and synaptic inhibition of mouse cerebellum lacking glutamate decarboxylase 67. Biochem. Biophys. Res. Commun. *370*, 429–433.

Olivo-Marin, J.-C. (2002). Extraction of spots in biological images using multiscale products. Pattern Recognit. *35*, 1989–1996.

Parsons, R.L., Calupca, M.A., Merriam, L.A., and Prior, C. (1999). Empty synaptic vesicles recycle and undergo exocytosis at vesamicol-treated motor nerve terminals. J. Neurophysiol. *81*, 2696–2700.

Poulain, B., Baux, G., and Tauc, L. (1986). Presynaptic transmitter content controls the number of quanta released at a neuro-neuronal cholinergic synapse. Proc. Natl. Acad. Sci. USA *83*, 170–173.

Riazanski, V., Deriy, L.V., Shevchenko, P.D., Le, B., Gomez, E.A., and Nelson, D.J. (2011). Presynaptic CLC-3 determines quantal size of inhibitory transmission in the hippocampus. Nat. Neurosci. *14*, 487–494.

Rizzoli, S.O., and Betz, W.J. (2005). Synaptic vesicle pools. Nat. Rev. Neurosci. *6*, 57–69.

Rizzoli, S.O., and Jahn, R. (2007). Kiss-and-run, collapse and 'readily retrievable' vesicles. Traffic *8*, 1137–1144.

Rothstein, J.D., Dykes-Hoberg, M., Pardo, C.A., Bristol, L.A., Jin, L., Kuncl, R.W., Kanai, Y., Hediger, M.A., Wang, Y., Schielke, J.P., and Welty, D.F. (1996). Knockout of glutamate transporters reveals a major role for astroglial transport in excitotoxicity and clearance of glutamate. Neuron *16*, 675–686.

Rousseau, F., Aubrey, K.R., and Supplisson, S. (2008). The glycine transporter GlyT2 controls the dynamics of synaptic vesicle refilling in inhibitory spinal cord neurons. J. Neurosci. *28*, 9755–9768.

Sara, Y., Mozhayeva, M.G., Liu, X., and Kavalali, E.T. (2002). Fast vesicle recycling supports neurotransmission during sustained stimulation at hippocampal synapses. J. Neurosci. *22*, 1608–1617.

Sepkuty, J.P., Cohen, A.S., Eccles, C., Rafiq, A., Behar, K., Ganel, R., Coulter, D.A., and Rothstein, J.D. (2002). A neuronal glutamate transporter contributes to neurotransmitter GABA synthesis and epilepsy. J. Neurosci. *22*, 6372–6379.

Solbu, T.T., Bjørkmo, M., Berghuis, P., Harkany, T., and Chaudhry, F.A. (2010). SAT1, a glutamine transporter, is preferentially expressed in GABAergic neurons. Front. Neuroanat *4*, 1.

Südhof, T.C. (2004). The synaptic vesicle cycle. Annu. Rev. Neurosci. *27*, 509–547.

Tabares, L., Alés, E., Lindau, M., and Alvarez de Toledo, G. (2001). Exocytosis of catecholamine (CA)-containing and CA-free granules in chromaffin cells. J. Biol. Chem. *276*, 39974–39979.

Tian, N., Petersen, C., Kash, S., Baekkeskov, S., Copenhagen, D., and Nicoll, R. (1999). The role of the synthetic enzyme GAD65 in the control of neuronal gamma-aminobutyric acid release. Proc. Natl. Acad. Sci. USA *96*, 12911–12916.

Tricoire, L., Pelkey, K.A., Erkkila, B.E., Jeffries, B.W., Yuan, X., and McBain, C.J. (2011). A blueprint for the spatiotemporal origins of mouse hippocampal interneuron diversity. J. Neurosci. *31*, 10948–10970.

Walls, A.B., Eyjolfsson, E.M., Smeland, O.B., Nilsen, L.H., Schousboe, I., Schousboe, A., Sonnewald, U., and Waagepetersen, H.S. (2011). Knockout of GAD65 has major impact on synaptic GABA synthesized from astrocyte-derived glutamine. J. Cereb. Blood Flow Metab. *31*, 494–503.

Wojcik, S.M., Rhee, J.S., Herzog, E., Sigler, A., Jahn, R., Takamori, S., Brose, N., and Rosenmund, C. (2004). An essential role for vesicular glutamate transporter 1 (VGLUT1) in postnatal development and control of quantal size. Proc. Natl. Acad. Sci. USA *101*, 7158–7163.

Wojcik, S.M., Katsurabayashi, S., Guillemin, I., Friauf, E., Rosenmund, C., Brose, N., and Rhee, J.S. (2006). A shared vesicular carrier allows synaptic corelease of GABA and glycine. Neuron *50*, 575–587.

Zhou, Q., Petersen, C.C., and Nicoll, R.A. (2000). Effects of reduced vesicular filling on synaptic transmission in rat hippocampal neurones. J. Physiol. *525*, 195–206.

Zucker, R.S., and Regehr, W.G. (2002). Short-term synaptic plasticity. Annu. Rev. Physiol. *64*, 355–405.